Modelling the adsorption of natural organic matter on Ag (111) surface: Insights from dispersion corrected density functional theory calculations

N.N. Nyangiwe[1,2]*, C.N.M Ouma[1,2]

[1]Natural Resources and the Environment, Council for Scientific and Industrial Research (CSIR), P O BOX 395, Pretoria, 0001, Republic of South Africa.
[2]University of Pretoria, Department of Chemical Engineering, Private Bag X 20, Hatfield, 0028, Republic of South Africa
[3]*HySA-Infrastructure, North-West University, Faculty of Engineering, Private Bag X6001, Potchefstroom, 2520, South Africa*

* Corresponding author. Natural Resources and the Environment, Council for Scientific and Industrial Research (CSIR), P O BOX 395, Pretoria, 0001, South Africa. nyangiwenangamso9@gmail.com

Highlights

• In both gas and water phase Cry showed stronger adsorption which means it has a stronger interaction with Ag (111) surface compared HA and FA.
• TDOS and PDOS indicated that indeed the chosen adsorbates do interact with the surface and are favourable on Ag (111) surface.
• Electrophilicity concur that charge transfer will take place from the adsorbates to Ag (111) surface.

Abstract

Understanding the nature of the interactions between natural organic matter (NOM) and engineered nanoparticles (ENPs) is of crucial importance in understanding the fate and behaviour of engineered nanoparticles in the environment. In the present study, dispersion-corrected density functional theory (DFT-D) has been used to elucidate the molecule-surface interactions of higher molecular weight (HMW) NOM ambiguously present in the aquatic systems, namely: humic acid (HA), fulvic acid (FA) and protein Cryptochrome (Cry) on Ag (111) surface. Investigations were done in the gas phase and to mimic real biological environment, water has been used as a solvent within the conductor-like screening model (COSMO) framework. The calculated adsorption energies for HA, FA and Cry on Ag (111) surface were -27.90 (-18.45) kcal/mol, -38.28 (-18.68) kcal/mol and -143.89 (-150.82) kcal/mol respectively in the gas (solvent) phase and the equilibrium distances between the surface and HA, FA and Cry molecules were 1.87 (2.18) Å, 2.31(2.31) Å and 1.91 (1.70) Å respectively in the gas (solvent) phase. In both gas and water phase Cry showed stronger adsorption which means it has a stronger interaction with Ag (111) surface compared to HA and FA. The results for adsorption energy, solvation energy, isosurface of charge deformation difference, total density of state and partial density of states indicated that indeed these chosen adsorbates do interact with the surface and are favourable on Ag (111) surface. In terms of charge transfer, one of many calculated descriptors in this study, electrophilicity (ω) concur that charge transfer will take place from the adsorbates to Ag (111) surface.

Keywords: *Interactions, humic acid, fulvic acid, cryptochrome, adsorption energy, DFT-D, NOM*

Graphical abstract

Figure G1: Charge density difference for (a) Ag (111)-HA, (b) Ag (111)-FA and (c) Ag (111)-Cry at DFT-D gas phase level of theory. The isovalue is taken as 0.009 au.

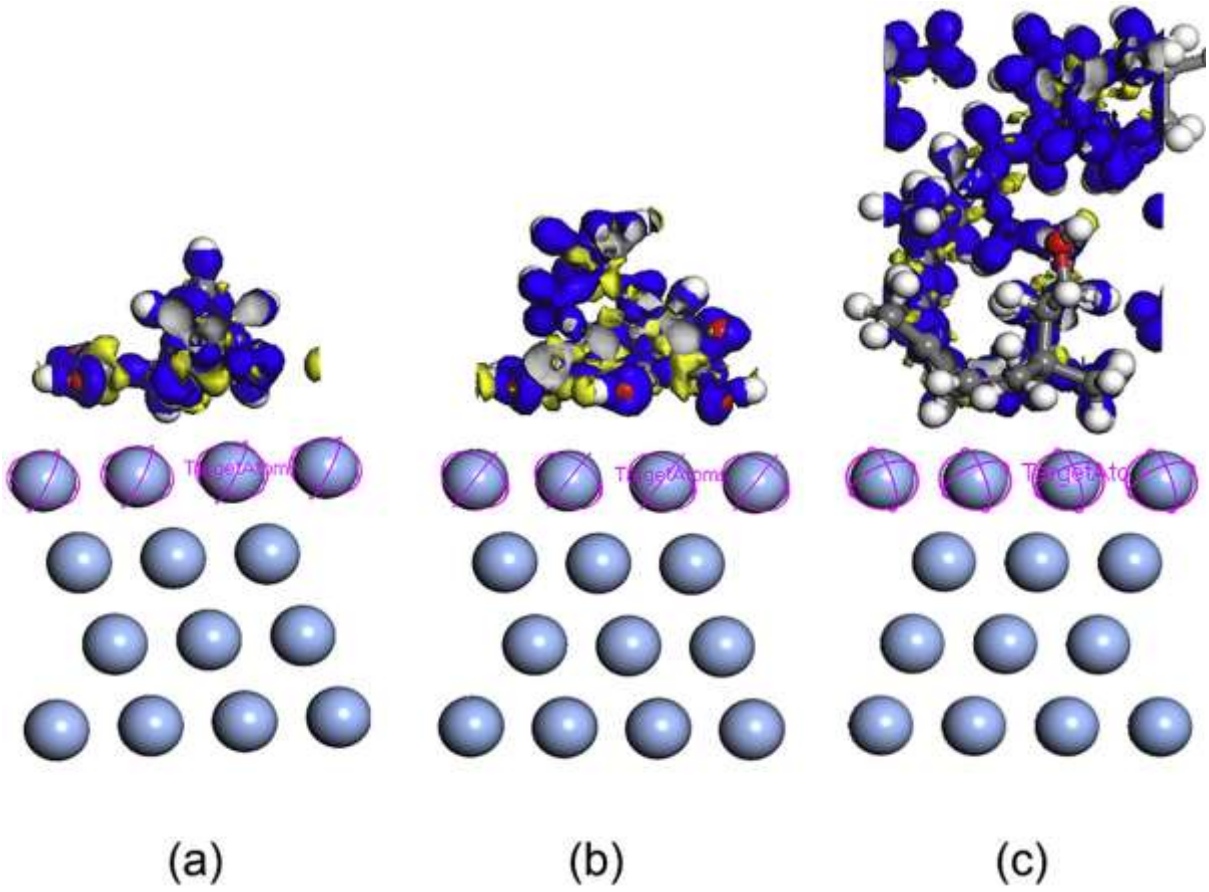

1. Introduction

Fundamental understanding of molecule-surface interactions has attracted lots of scientific attention both theoretically and experimentally [1],[2].These scientific efforts have mainly been focused on gaining valuable information on how these molecule-surface interactions influence the surface intrinsic properties of different of engineered nanoparticles [3-5]. Surface studies have resulted in numerous technological applications, for example, in clean energy, electronics, and biological applications [6-8]. Further, with dramatic advances in technological and technical capabilities over the last two decades most metals and metal-oxides have been used as precursors in the production of engineered nanoparticles (ENPs) [9],[10]. ENPs are characterised by unique optical electronic and catalytic properties [11], among others, and therefore exhibits distinctive characteristics from their bulk counterparts [12-14]. Nowadays, ENPs are widely used in textiles, food packaging, cosmetics, medical devices, and household appliances [15],[16]. These applications have resulted in ENPs constituting a new class of emerging pollutants [17] due their continued release into the environment. Since their potential impacts are relatively unknown [18],[19], there are serious concerns being raised on their impact [20],[21]. In pursuit to elucidate the fate and effects of ENPs in the environment, natural organic matter (NOM) has been identified to be among the key influencing factors on the

stability of ENPs in the environment [22],[23]. Therefore, it is essential to gain fundamental understanding on interactions mechanisms of different NOM with ENPs since they control the degree of ENPs stability in the aquatic systems [24],[25]. As yet, theoretical studies (DFT and/or MD) on insights at a fundamental level on ENP-NOM interactions are still limited in comparison to experimental studies available in literature hence the focus of this study.

Experimentally [26], the interaction between natural organic matter (NOM) with ENPs, have been characterized by techniques such as ;(1) Zeta potential analysis (ζ), however despite all the merits of this technique, it still cannot provide direct information on the surface interaction, it can only help elucidate the adsorption mechanism;(2) Isothermal titration calorimetry (ITC) which measures the association process between NOM and ENPs in a numerical process;(3) Size exclusion chromatography (SEC) which is regarded as a simple, quick and relatively cheap method however it gives no further information on the adsorption mechanism [26]; (4) Nuclear magnetic resonance (NMR) which is sensitive and dependable and can offer valuable evidence on structure changes induced by ENP–NOM interactions, however it is somewhat expensive [26]. To the best of the authors knowledge, at the moment, there is no single approach that covers all the information on the complex interaction between NOM and ENPs. Even though a lot has been done experimentally, observations do not fully account for the binding characteristics of ENPs and NOM and hence the need to apply first principles calculations proposed herein in addressing this problem as highlighted previously [27]. Evaluation of the fate and behaviour of ENPs is necessary in order to design products that are safe, and functions without inducing undesirable biological effects in the aquatic systems [28]. There is need to develop computational models to serve as a first-tier screening tool to predict the fate and behaviour of ENPs in the aquatic systems since to some extent experimental fate studies are usually not only laborious, time-consuming but are also resource-intensive.

In this study, within the dispersion corrected density functional theory formalism (DFT-D), the Ag (111) surface, as prototype ENP surface, was used to investigate surface-NOM interaction with three representative high molecular weight (HMW) NOMs namely; humic acid, fulvic acid and cryptochrome widely found in the aquatic systems. By definition, low molecular weights (LMW) imply molecules whose molecular weight is less than 2000 Da and HMW imply molecules whose molecular weight ranges from 2000 Da up to 10,000 Da, and the molecule contains numerous functional groups, such as thiols, phenolic-OH, quinones, aldehydes, ketones, carboxyls and methoxyls [29]. The Ag (111) surface was chosen based on a previous *ab initio* study where it was found to be most stable [27]. Ag has high metal density (14 Ag/nm2) [30], and therefore, has high reactivity [30]. From an earlier study, a linear direct relationship between the molecular weight (MW) of NOMs and the adsorption energies was established [15], where adsorption energy was shown to increase as the MW increased. Further, using the frontier molecular orbital (FMO) theory calculations, a direct relationship between the dipole moment, molecular surface area, absolute electronegativity, absolute hardness and the molar mass of the adsorbate for low MW NOMs (< 200 Da) was also established [27].

In this work we study the interaction between fulvic acid, humic acid and cryptochrome and Ag (111) surface, the study provides critical understanding of the NOM-Ag (111) interactions, which is crucial in understanding the fate, and behaviour of ENPs in the environment. A clear understanding of fate and behaviour of engineered nanoparticles in the environment is still an ongoing discussion; thus this study seeks to contribute in that discussion. In order to understand these NOM-Ag (111) interactions, the following have been calculated: adsorption energy, solvation energy, charge deformation difference, highest occupied molecular orbital (HOMO), lowest unoccupied molecular orbital (LUMO), energy gap (Eg), chemical potential (μ), ionization potential (I), electron affinity (A), electronegativity (χ), hardness (η) and electrophilicity (ω). To investigate the electronic structure properties of fulvic acid, humic acid and cryptochrome on Ag (111) surface, total density of states (TDOS) and projected density of states (PDOS) analysis were calculated.

2. Computational details

All calculations were performed using the DFT-D [31],[32] approach as implemented in the DMol3 [33] within the Materials Studio BIOVIA [34]. DFT-D was used to accurately account for the van der Waals (vdW) interactions between the NOM and Ag (111) surface [31]. The generalized gradient approximation (GGA) method as proposed by Perdew and Wang (PW91) was used to approximate the exchange–correlation functional [35] as it provides better overall description of the electronic system [36] and the double-numerical quality basis set with polarization functions (DNP) were employed [37].

DFT semi-core pseudopotential (DSPP) was set to account for relativistic effects to balance calculation accuracy and computational efficiency [38]. Ag (111) surface was modelled by a slab consisting of four layers repeated in a 4x4 surface unit cell with a separation of 15 Å between clean slabs to ensure no interactions between the sorbate and its periodic image. Uppermost two layers of the Ag atoms were relaxed along with the adsorbates, and the remaining substrate layers were constrained. The optimized geometrical structure of model Ag (111) surfaces used to adsorb the NOMs are shown in Figure 1. Gamma point *k*-point sampling was used and a real-space cut-off radius was maintained at 4.5 Å to improve the computational performance [37]. The electronic energy convergence criteria, gradient, and atom displacement, were set as 0.00001 Ha (Ha is hartree), 0.002 Ha/Å, and 0.005 Å, respectively. To accelerate convergence speed of charge density of self-consistent field calculation time, and also enhance efficiency, direct inversion of iterative subspace (DIIS) was used.

To model the solvation effects in water, where electrostatic interactions of solutes with solvent are taken into account, solvation calculations on Ag (111) surface, fulvic acid, humic acid and cryptochrome complexes were performed using the conductor-like screening model (COSMO) as implemented in DMol3 [39]. The continuum solvation model, COSMO, was selected since it is both simple and computationally efficient in comparison with explicit solvent phase simulations [40]. It also aids in the prediction of physicochemical properties of chemical species in solution media [41],[42]

with the goal of generating results valuable to experimentalists [43]. In this study, water with permittivity (ε) = 78.4 was chosen as solvent primarily to mimic the interactions of ENPs with different NOMs defined by wide variations of MWs present in the aquatic systems. Figure 1 shows optimized geometries of Ag (111) surface with the respective adsorbates.

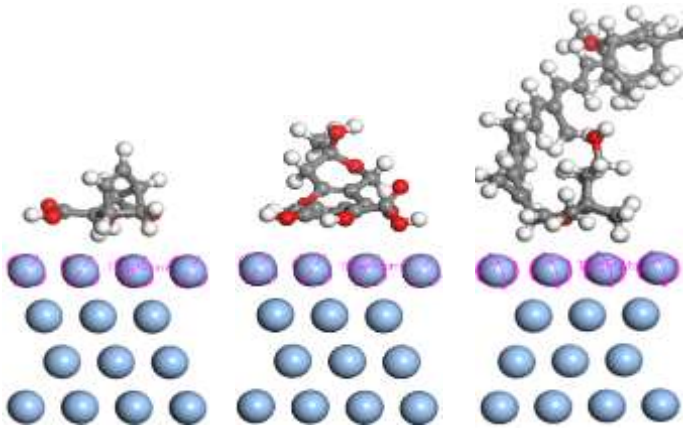

(a (b) (c)

Figure 1: Optimized geometrical structures and relaxed configurations of (a) HA, (b) FA and (c) Cry molecules adsorbed on Ag (111) surface (color code; oxygen: red, grey: carbon, white: hydrogen).

From Figure 1 (a) and (c), it is evident that humic acid and cryptochrome adsorption occurred through its hydrogen atom facing the Ag (111) surface while for the fulvic acid (Figure 1(b)) adsorption occurred through one oxygen in the carbonyl group, and hydrogen atom. The calculated adsorption energies listed in Table 1,were obtained using equation 1.1

$$Eads = E_{(surf+adsorbate)} - E_{surf} - E_{adsorbate} + \text{BSSE} \quad (1.1)$$

3. Results and discussion

Interest in adsorption of fulvic acid, humic acid and cryptochrome on Ag (111) surface stems from the fact that NOMs substantially modify the physical and chemical properties of the surface by accepting (donating) electrons [44].The results in Table1 show that the adsorption of fulvic acid, humic acid and cryptochrome is energetically favourable since only negative adsorption energy values were obtained.

Table 1: Adsorption energies (kcal/mol) and the equilibrium distance between NOM's and Ag (111) surface.

System	E_{ads} (kcal/mol)	$d_{H\text{-}Ag}$ (Å)
Gas phase		
Ag (111)-HA	-27.90	1.87
Ag (111)-FA	-38.28	2.31
Ag (111)-Cry	-143.89	1.91
COSMO (Water)		
Ag (111)-HA	-18.45	2.18
Ag (111)-FA	-18.68	2.31
Ag (111)-Cry	-150.59	1.70

According to [45] the NOM's can interact with Ag (111) surface via several different ways by utilizing H, N atoms and O lone pair electrons. The chemical formula for fulvic acid, humic acid and cryptochrome are ($C_9H_9NO_6$), ($C_{14}H_{12}O_8$) and ($C_{40}H_{56}O_3$), the strong interaction as shown by the highest adsorption of Cry can be attributed to fact that it has many carbon and hydrogen atoms interacting with the Ag (111) surface. As observed by [46] the adsorption energy is maximum for larger sized cryptochrome this can be explained on the basis of fundamentals of Van der Waals forces that are directly proportional to the size and mass of the interacting molecules [46]. From Table 1 has the second strongest interaction that can also be attributed to the fact that it has the highest number of carbon, hydrogen and oxygen atoms interacting with the surface. The higher the adsorption energy, the stable the molecule. Similar conclusion was observed by [47] while working on interaction of inhibitor with Fe (110) surface. Chemahini and co-workers [48] while working on the interaction between lactic acid and single-wall carbon nanotubes arrived to same conclusion. It is evident from the Table 1 that moving from gas phase to water the adsorption energy values of humic acid and fulvic acid decrease, while the adsorption energy value for cryptochrome moving from gas phase to water phase increase. In the case of humic acid and fulvic acid water did not enhance adsorption or make the interaction between the NOM and Ag (111) surface. A previous study by [48] reported decreasing and increasing adsorption energies values moving from gas phase to water while working on the interaction between lactic acid and single-wall carbon nanotubes.

Experimental results have shown that adsorbed NOM molecules with high MW could introduce steric repulsion and prevent the direct contact between ENPs and cells/organisms, thus decreasing the toxicity of ENPs [24] thus, an NOM is expected to attach to the surface of ENPs which in turn may change their physiochemical properties and the interfacial forces or energies between interacting ENPs thereby, altering the ENPs' aggregation behaviour [24]. Stronger NOM-surface interaction by means of adsorption energies indicate that in the environment the NOM is likely to stay longer attached to the ENPs, whereas in the case of weak NOM-surface interaction, the NOM is likely to separate from the ENPs because of weak adsorption energy. Once NOM detaches from the ENP's surface, a process of dissolution takes place resulting in the release of silver ions [49] hence the importance of the NOM binding strongly to the ENP surface.

The energy needed to move a molecule from its gas to solvent phase is referred to as the solvation energy. The results presented in the text below were calculated using equation 2.1

$$\Delta E_{solvation} = E_{water} - E_{gas} \quad (2.1)$$

Ag (111)-HA (-3.69 kcal/mol), Ag (111)-FA (-5.30 kcal/mol) and Ag (111)-Cry (-23.98 kcal/mol) respectively. As seen from the solvation energy values, a direct relationship between the calculated $\Delta E_{solvation}$ and the molecular weights of the NOMs was also observed. The solvation energy results followed a similar trend to those of adsorption energy. The molecular weight is the contributing factor.

3.1 Analysis of density of states (DOS)

To better understand the interactions between Ag (111) surface and adsorbates the electronic properties were studied using the total density of states (TDOS) especially near the Fermi level. In Figure 2 (a-c), results for TDOS of pristine alone, adsorbates alone and Ag (111) surface with adsorbates calculated using DFT-D/GGA in gas phase and in water as a solvent are summarised. From TDOS plot in Figure 2 (a), the pristine Ag (111) surface show peaks at and above Fermi level, which is typical for metals. The TDOS plots for humic acid and fulvic acid were found to be very similar as both adsorbates are humic substances; where the peaks observed below Fermi level and above Fermi level were at the same energy positions between -9.9 and -0.4 eV below the Fermi level, and 0.4 eV and 4.4 eV above Fermi level (Figure 2 (b)). In the case of cryptochrome, fewer peaks were observed below and above the Fermi level. Following adsorption of adsorbates on Ag (111) surface, the calculated TDOS for the adsorbed systems were observed to be relatively similar to that of pristine Ag (111) surface in the energy range -8 to 5 eV. This indicates that around the Fermi level, the adsorbates had no significant influence on the electronic properties of Ag (111) surface based on TDOS analysis. Previous study showed that the total DOS of Cu (1 1 1) after C3F7CN adsorption has some change, which is manifested by the increased DOS near the range from −6 eV to −8 eV [50]. The adsorption of NOM's on Ag (111) surface can substantially modify the physical and chemical properties of molecules and enhance the stability of the system by accepting the electrons from antibonding states [44].

Projected density of states (PDOS) plots for the surface alone, adsorbates alone and Ag (111) surface with adsorbates calculated using DFT-D/GGA in gas phase and in water as a solvent are shown in Figures S2-S3. Further, to gain insights on NOM-Ag (111) surface electronic properties PDOS was done. Only the *s* and *p* orbitals were considered because silver is a transition metal where *d* and *f* orbitals are (semi) filled. In Figures S1 (a-b), the PDOS of humic acid, fulvic acid, cryptochrome, Ag (111) surface pristine, and humic acid, fulvic acid, cryptochrome, Ag (111) surface in gas phase and COSMO have been shown.

The PDOS values of s- and p-, and-orbitals are all decreased after adsorption both in gas and water phase (Figure S5). It suggests that NOM's have influence towards the orbitals of Ag (111) formed bond interaction, similar observations were reported by [51]. In turn, the adsorption process is enhanced. The change shows distinct change in all orbitals indicating a strong bond interaction. In conclusion, the strong orbital hybridization among humic acid, fulvic acid and cryptochrome atoms orbitals stabilizes the adsorption of Ag (111) surface. For comparison both TDOS and PDOS pristine Ag (111) surface, humic acid on Ag (111) surface and fulvic acid on Ag (111) surface are drawn from -10 eV to 5 eV, this was done to show the electronic states around the Fermi level.

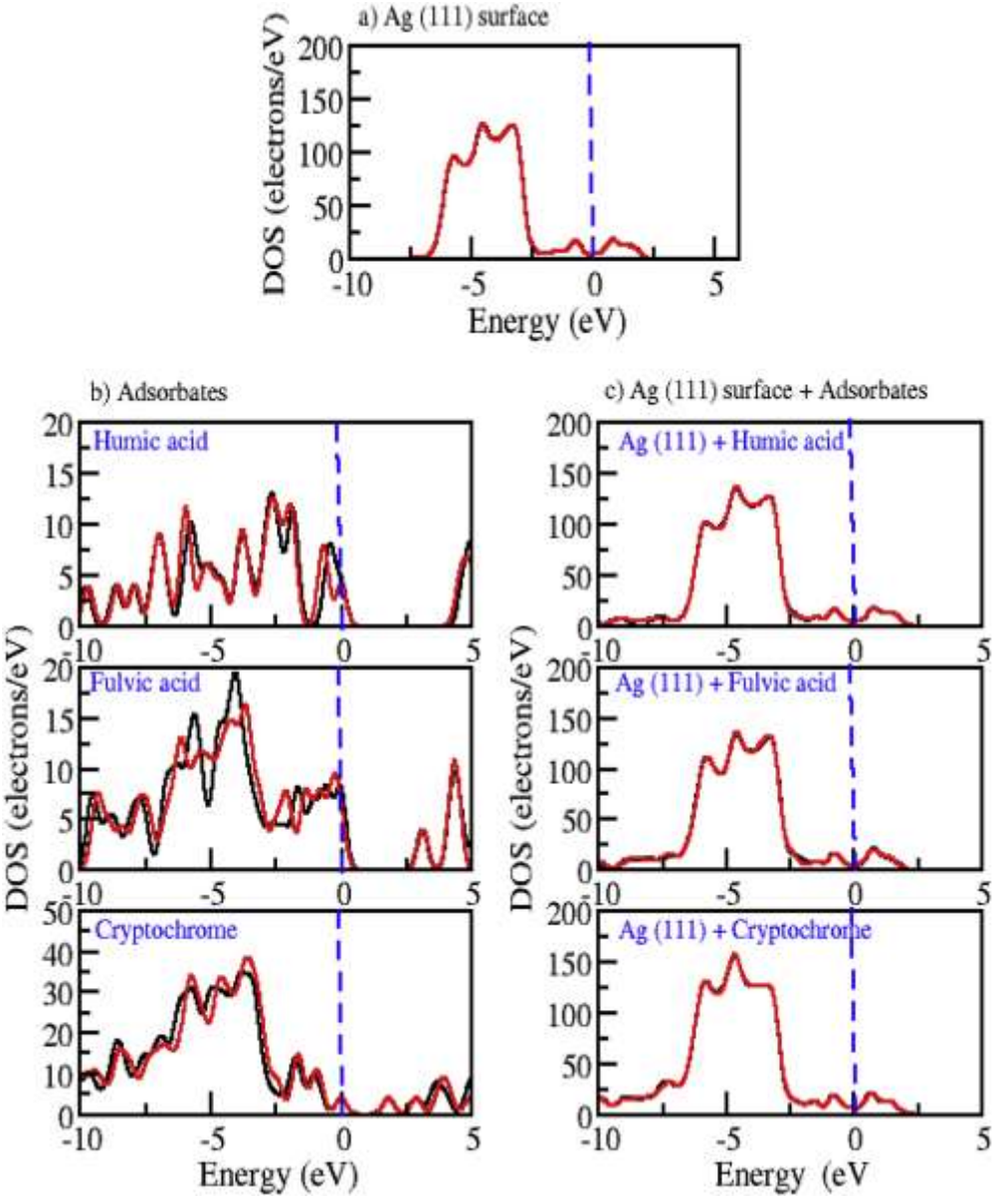

Figure 2: The TDOS calculated using DFT-D/GGA formalism for adsorbed HA, FA and Cry in gas and water as a solvent.

3.2 Quantum chemical calculations

It is a known fact that the bonding interaction between molecules and metal surface relies on the frontier orbital energetic position and the Fermi energy of metal [52]. The quantum chemical descriptors have been calculated to understand the properties of the studied molecules that could be used as possible inputs in creating either a (QSAR) or (QSPR) needed for the development of ENP toxicity model. The most commonly investigated descriptors for QSAR include (HOMO), (LUMO), HOMO-LUMO gap (Eg) which were also calculated in this study [53],[48].

Several studies have confirmed that the reactivity of a molecule depends on the molecular orbital distribution [54],[55]. HOMO regularly indicates the electron donating ability of a molecule, while LUMO is associated with its ability to accept electrons [56],[57]. The molecular structures of these three adsorbates and the frontier molecule orbital density distributions are shown in Figures S10-S11 (supporting document). It is seen that the HOMO of HA is mostly distributed on the C-H atoms indicating that it is the C-H bonds which will most likely donate electrons to the surface while the HOMO of fulvic acid and cryptochrome is distributed throughout the inner atoms and indications that for these adsorbates all atoms will donate electrons to the surface. The HOMO distributions of humic acid, fulvic acid and cryptochrome molecules have been plotted in Figures S10-S11. It had been previously reported [58] that ω is a descriptor that could indicate the direction of charge transfer. The higher the value of ω, the higher the electrophilic power of the investigated structure [58]. From Table 2, the electrophilicity index values of humic acid, fulvic acid and cryptochrome in both gas and water phases are lower than that of Ag (111) surface, indicating that there will be a charge transfer from these molecules to Ag (111) surface. It is worth noting that higher adsorption energy and narrow HOMO-LUMO energy gap suggest a strong binding interaction of the cryptochrome molecule to Ag (111) and this can be attributed to its hydrophilicity. From Table 3, results indicate that all the adsorbates before and after the adsorption on Ag (111) surface exhibit very similar values of HOMO and LUMO.

Before adsorption in the gas phase the HOMO values for humic acid, fulvic acid and cryptochrome were -5.97, -5.48 and -4.25 eV respectively. Still in the gas phase the HOMO values after adsorption for humic acid, fulvic acid and cryptochrome were -5.31, -5.08 and -5.09 respectively. The HOMO values in water for humic acid, fulvic acid and cryptochrome were –6.02, -5.77 and -4.57 eV before adsorption, after adsorption the humic acid, fulvic acid and cryptochrome HOMO values changed to -5.38, -5.24 and -5.40 eV respectively. In the case of LUMO values before adsorption in the gas phase for humic acid, fulvic acid and cryptochrome were -1.28, -2.38, -2.44 eV respectively. After adsorption in the gas phase the LUMO for humic acid, fulvic acid and cryptochrome changed to -4.90, -4.69 and -5.04 eV respectively. The LUMO values in water before adsorption for humic acid, fulvic acid and cryptochrome were -1.47, -2.63 and -2.76 eV respectively, after the adsorption the LUMO values for humic acid, fulvic acid and cryptochrome changed to -4.97, -4.84 and -5.16 eV respectively. The higher value of HOMO and the lower value of LUMO indicate a tendency of the molecule to donate

and accept electrons, respectively [59]. A less negative HOMO energy (E_{HOMO}) gives more charges to unfilled d orbitals of Ag (111) surface, while a LUMO (E_{LUMO}) containing smaller energy could easily receive more electrons.

The HOMO and LUMO values show noticeable changed after the adsorption of NOM's on the Ag (111), these results are consistent to what was reported by [47]. As shown in Table 3, the Eg values of isolated humic acid, fulvic acid and cryptochrome molecules are 4.69, 3.10 and 1.81 eV respectively in gas phase, after the adsorption on Ag (111) surface, the Eg values changed to 0.41, 0.39 and 0.05 eV respectively confirming the interaction, similar observation was noticed also in the water phase. This suggests that a decreased energy gap gives rise to an intensified charge sharing at interface of humic acid, fulvic acid and cryptochrome and Ag (111) surface, which in turn brings about strengthened interactions [60]. The energy gap Eg is often assumed to prompt the chemical reactivity of the NOM molecules toward the substrate surface. Some scholars contemplate that a low Eg value ordinarily corresponds to a high NOM efficiency in the NOM molecule [61],[62]. In another study [63] argue that, the factors that affect NOM efficiency are multifarious, for example, the molecule absorption location is subtle to the dipole–dipole interaction. Also Hahn [64] reported that the energy gap of pyridine molecule decreases about 0.9 eV while interacting with Ag(110) surface. One way of clarifying this is that the charging process of the top most metal surface appeared to affect the electronic structure of the adsorbate in such a way that its molecular orbitals were fully stabilized by adsorption [47]. Previous study by [50], obtained similar result and arrived to a similar conclusion that the energy of the HOMO is found to be higher (Table 3), while that of the LUMO is lower under the influence of high dielectric environment, resulting in lowering of the HOMO-LUMO gap. This is consistent with what was observed elsewhere [50]. It is evident from Table 3 that the adsorption of NOM's reduces the energy gap, this has been reported by [47] before.

Table 2: Calculated global reactivity descriptors in COSMO at DFT-D/GGA level of theory.

		DFT-D Gas phase (eV)					DFT-D COSMO (eV)				
System	MW (g/mol)	I	A	χ	η	Ω	I	A	χ	η	ω
HA	226.16	5.97	1.28	3.63	2.34	2.81	6.02	1.47	3.74	2.28	3.08
FA	308.24	5.48	2.38	3.93	1.55	2.98	5.77	2.63	4.20	1.57	5.63
Cry	584.88	4.25	2.44	3.34	0.91	6.16	4.57	2.76	3.66	0.91	7.40
Ag (111)	-	5.38	4.85	5.12	0.27	49.35	5.39	4.86	5.13	0.27	49.50
Ag (111) –HA	-	5.31	4.90	5.10	0.21	63.39	5.38	4.97	5.17	0.21	64.70
Ag (111) –FA	-	5.08	4.69	4.88	0.20	60.43	5.24	4.84	5.04	0.20	62.22
Ag (111) –Cry	-	5.09	5.04	5.06	0.02	523.57	5.40	5.16	5.28	0.12	115.13

Table 3: Calculated global reactivity descriptors in the gas phase at DFT-D/GGA level of theory.

		DFT-D Gas phase (eV)				DFT-D COSMO (eV)			
System	MW*	E_{HOMO}	E_{LUMO}	Eg	μ	E_{HOMO}	E_{LUMO}	Eg	μ
HA	226.16	-5.97	-1.28	4.69	-3.63	-6.02	-1.47	4.55	-3.74
FA	308.24	-5.48	-2.38	3.10	-3.93	-5.77	-2.63	3.14	-4.20
Cry	584.88	-4.25	-2.44	1.81	-3.34	-4.57	-2.76	1.82	-3.66
Ag (111)	-	-5.38	-4.85	0.53	-5.12	-5.39	-4.86	0.53	-5.13
Ag (111) –HA	-	-5.31	-4.90	0.41	-5.10	-5.38	-4.97	0.41	-5.17
Ag (111) –FA	-	-5.08	-4.69	0.39	-4.88	-5.24	-4.84	0.41	-5.04
Ag (111) –Cry	-	-5.09	-5.04	0.05	-5.06	-5.40	-5.16	0.24	-5.28

*MW expressed in g/mol

Among all systems, it can be seen that the cryptochrome had the highest electrophilicity index which means cryptochrome has highest reactivity among all systems. This observation implies a direct relation with adsorption energy as well as molecular weight. The results of other calculated global reactivity descriptors presented in Tables 2 and 3 show that while going from the gas phase to water the HOMO, LUMO, μ, I, χ and ω increase while Eg, A and η values in some cases vary or remain unchanged. While working on Carbon Nanotubes [48] also made a similar observation that, electrophilicity increases going from the gas phase to the solvent phase. Previous studies [65],[66] have also shown that lower Eg means higher electrical conductivity and in contrast higher Eg corresponds to the lower electrical conductivity. It can be concluded that for all systems, cryptochrome has higher electrical conductivity than humic acid and fulvic acid.

The η of Ag (111) decreases upon the adsorption of humic acid, fulvic acid and cryptochrome decreases, from Table 2, the decrease in hardness of Ag (111) surface upon adsorption is in order of humic acid > fulvic acid > cryptochrome, these results were consistent as they increased going from gas phase to solvent.. If the μ value is negative, it means that the compound is stable and can exist in this configuration [67]. The calculated chemical potential and electronegativity values in Tables 2 and 3 for the humic acid, fulvic acid and cryptochrome show that after the adsorption on Ag (111) surface, the chemical potential for HA, FA and Cry increased from -3.63, -3.93 and -3.34 respectively before adsorption to -5.10, -4.88 and -5.06 respectively after adsorption. The increase was consistent in both gas phase and water as the solvent and a trend was observed where μ values increased moving from gas phase to solvent.

3.3 Structure and charge analysis

The effect of humic acid, fulvic acid and cryptochrome adsorption on Ag (111) surface has been investigated by plotting the charge deformation difference (provided in supporting document). In Table S1 and Figure S4, structural properties and charge deformation difference of adsorbates are shown. The interatomic bonds of the humic acid, fulvic acid and cryptochrome molecules were calculated and compared before and after relaxation as summarized in Table S1. From the results small differences

were noted for bond distances before and after relaxation. To the authors' knowledge, no previous theoretical and experimental studies on reported bond lengths of humic acid, fulvic acid and cryptochrome hence no comparison were made on this.

To better understand the distribution patterns of charges around the adsorbates, the charge density difference at the interface between the adsorbate and the surface were plotted in three-dimensional (3D) (see Figure S4). For the fulvic acid and cryptochrome shown in Figure S4 (b) and (c), respectively, a strong redistribution of charges between C=O, C-C, C-H and -OH group was observed, and possibly could yield a change in electronic structure. The 3D iso-surfaces Figure S4 (b-d) of Ag (111)-humic acid, Ag (111)-fulvic acid and Ag (111)-cryptochrome at the interface indicate that the charge was localized mostly on the humic acid, fulvic acid, and cryptochrome with smaller amounts on the pristine Ag (111) surface as shown in Figure S1 (a). In addition, results in Figures S5-S7 (a) clearly show that regions with oxygen atom had higher charges, and hence the functional group likely to exert strong influence on the Ag (111) surface. The electron density difference show the strong interaction between humic acid, fulvic acid and cryptochrome Ag (1 1 1) surface. The isosurface charge density difference for (a) Ag (111) pristine, (b) Ag (111)-humic acid, (c) Ag (111)-fulvic acid and (d) Ag (111)-cryptochrome were the same irrespective of formalism used to perform the calculations (Figures S8-S11).

4. Conclusion

Dispersion correction density functional theory (DFT-D) has been used to gain insight on the adsorption of high molecular weight natural organic matter with Ag (111). The calculated adsorption energy indicates that the adsorption was spontaneous and exothermic. The calculated solvation energies indicate that the adsorbates are stable while in solution and there was a direct relation between the adsorbate's molecular weight and the calculated solvation and adsorption energies. From the calculated adsorption energies it can be concluded that fulvic acid and cryptochrome will strongly bind to the ENP surface and reside longer in the environment in comparison to humic acid implying that fulvic acid and cryptochrome can stabilize the ENP longer than humic acid would. Total density of states of Ag (111) surface, humic acid, fulvic acid, cryptochrome, humic acid on Ag (111), fulvic acid on Ag (111) and cryptochrome on Ag (111) surface have been plotted. TDOS is drawn from -10 eV to 5 eV, this was done to show the electronic structures near the Fermi level. The global reactivity descriptors such as HOMO LUMO, Eg, μ, I, A, χ, η and ω were calculated. The results of calculated global reactivity descriptors show that while going from the gas phase to water the HOMO, LUMO, chemical potential, ionization potential, electronegativity and electrophilicity values increased, while Eg, A and η values in some cases vary or remain unchanged, that has been shown by DFT-D level of theory.

Acknowledgments

The authors acknowledge funding from the National Research Foundation (N.N.Nyangiwe), Council for Scientific and Industrial Research (N.N. Nyangiwe, C.N. Ouma). The computing and simulation resources from the Centre for High Performance Computing (CHPC), South Africa, are acknowledged.

References

[1] G.C. Sosso, R.J. Maurer, Computational Molecular Science, (2019).

[2] M.T.A.N. Mudiyans, Fundamental Surface Properties and Gas-Surface Interactions of Two-Dimensional Materials, North Dakota State University, 2019.

[3] Z. Ding, Y. Jiao, S. Meng, Quantum simulation of molecular interaction and dynamics at surfaces, Front. Phys. 6 (2011) 294–308.

[4] A. Li, J.-P. Piquemal, J. Richardi, M. Calatayud, Butanethiol adsorption and dissociation on Ag (111): A periodic DFT study, Surf. Sci. (2015).

[5] K.M. Bal, E.C. Neyts, Overcoming Old Scaling Relations and Establishing New Correlations in Catalytic Surface Chemistry: Combined Effect of Charging and Doping, J. Phys. Chem. C. (2019).

[6] J. Lahtinen, A. Vehanen, Applications of positron techniques to surface studies and catalysis, Catal. Letters. 8 (1991) 67–100.

[7] D.P. Woodruff, Modern techniques of surface science, Cambridge university press, 2016.

[8] D.P.R. Thanu, M. Zhao, Z. Han, M. Keswani, Fundamentals and Applications of Sonic Technology, in: Dev. Surf. Contam. Clean. Appl. Clean. Tech., Elsevier, 2019: pp. 1–48.

[9] S. Pocov\í-Mart\ínez, D. Cassano, V. Voliani, Naked Nanoparticles in Silica Nanocapsules: A Versatile Family of Nanorattle Catalysts, ACS Appl. Nano Mater. 1 (2018) 1836–1840.

[10] M.F. Hochella, D.W. Mogk, J. Ranville, I.C. Allen, G.W. Luther, L.C. Marr, B.P. McGrail, M. Murayama, N.P. Qafoku, K.M. Rosso, others, Natural, incidental, and engineered nanomaterials and their impacts on the Earth system, Science (80-.). 363 (2019) eaau8299.

[11] R.D. Adams, B. Captain, L. Zhu, Platinum participation in the hydrogenation of phenylacetylene by Ru5 (CO) 15 (C)[Pt (PBut3)], J. Am. Chem. Soc. 126 (2004) 3042–3043.

[12] Z.-J. Jiang, C.-Y. Liu, L.-W. Sun, Catalytic properties of silver nanoparticles supported on silica spheres, J. Phys. Chem. B. 109 (2005) 1730–1735.

[13] T.E.G. Alivio, N.A. Fleer, J. Singh, G. Nadadur, M. Feng, S. Banerjee, V.K. Sharma, Stabilization of Ag--Au Bimetallic Nanocrystals in Aquatic Environments Mediated by Dissolved Organic Matter: A Mechanistic Perspective, Environ. Sci. Technol. 52 (2018) 7269–7278.

[14] M. Swaminathan, N.K. Sharma, Antimicrobial Activity of the Engineered Nanoparticles Used as Coating Agents, Handb. Ecomater. (2019) 549–563.

[15] T. V Duncan, K. Pillai, Release of engineered nanomaterials from polymer nanocomposites: diffusion, dissolution, and desorption, ACS Appl. Mater. Interfaces. 7 (2014) 2–19.

[16] K. Kumari, P. Singh, K. Bauddh, S. Mallick, R. Chandra, others, Implications of Metal

Nanoparticles on Aquatic Fauna: A Review, Nanosci. Nanotechnology-Asia. 9 (2019) 30–43.

[17] M.J. Eckelman, M.S. Mauter, J.A. Isaacs, M. Elimelech, New perspectives on nanomaterial aquatic ecotoxicity: production impacts exceed direct exposure impacts for carbon nanotoubes, Environ. Sci. Technol. 46 (2012) 2902–2910.

[18] C.M. Rico, S. Majumdar, M. Duarte-Gardea, J.R. Peralta-Videa, J.L. Gardea-Torresdey, Interaction of nanoparticles with edible plants and their possible implications in the food chain, J. Agric. Food Chem. 59 (2011) 3485–3498.

[19] B. Huang, Z.-B. Wei, L.-Y. Yang, K. Pan, A.-J. Miao, Combined Toxicity of Silver Nanoparticles with Hematite or Plastic Nanoparticles toward Two Freshwater Algae, Environ. Sci. Technol. (2019).

[20] A.B.A. Boxall, D.W. Kolpin, B. Halling-Sørensen, J. Tolls, Peer reviewed: are veterinary medicines causing environmental risks?, (2003).

[21] Y. Zhu, J.R. Snape, K.C. Jones, A.J. Sweetman, Spatially explicit large-scale environmental risk assessment of pharmaceuticals in surface water in China, Environ. Sci. Technol. (2019).

[22] V.K. Sharma, J. Filip, R. Zboril, R.S. Varma, Natural inorganic nanoparticles--formation, fate, and toxicity in the environment, Chem. Soc. Rev. 44 (2015) 8410–8423.

[23] M.C. Surette, J.A. Nason, Nanoparticle aggregation in a freshwater river: the role of engineered surface coatings, Environ. Sci. Nano. (2019).

[24] Z. Wang, L. Zhang, J. Zhao, B. Xing, Environmental processes and toxicity of metallic nanoparticles in aquatic systems as affected by natural organic matter, Environ. Sci. Nano. 3 (2016) 240–255.

[25] V.K. Sharma, C.M. Sayes, B. Guo, S. Pillai, J.G. Parsons, C. Wang, B. Yan, X. Ma, Interactions between silver nanoparticles and other metal nanoparticles under environmentally relevant conditions: A review, Sci. Total Environ. 653 (2019) 1042–1051.

[26] S. Yu, J. Liu, Y. Yin, M. Shen, Interactions between engineered nanoparticles and dissolved organic matter: A review on mechanisms and environmental effects, J. Environ. Sci. (2017).

[27] N.N. Nyangiwe, C.N. Ouma, N. Musee, Study on the interactions of Ag nanoparticles with low molecular weight organic matter using first principles calculations, Mater. Chem. Phys. (2017).

[28] R.S. Kookana, A.B.A. Boxall, P.T. Reeves, R. Ashauer, S. Beulke, Q. Chaudhry, G. Cornelis, T.F. Fernandes, J. Gan, M. Kah, others, Nanopesticides: guiding principles for regulatory evaluation of environmental risks, J. Agric. Food Chem. 62 (2014) 4227–4240.

[29] Y. Wang, M. Ye, R. Xie, S. Gong, Enhancing the In Vitro and In Vivo Stabilities of Polymeric Nucleic Acid Delivery Nanosystems, Bioconjug. Chem. 30 (2018) 325–337.

[30] J.C. Azcárate, G. Corthey, E. Pensa, C. Vericat, M.H. Fonticelli, R.C. Salvarezza, P. Carro, Understanding the Surface Chemistry of Thiolate-Protected Metallic Nanoparticles, J. Phys. Chem. Lett. 4 (2013) 3127–3138.

[31] F. Ortmann, F. Bechstedt, W.G. Schmidt, Semiempirical van der Waals correction to the density functional description of solids and molecular structures, Phys. Rev. B. 73 (2006) 205101.

[32] A. Tkatchenko, M. Scheffler, Accurate molecular van der Waals interactions from ground-state electron density and free-atom reference data, Phys. Rev. Lett. 102 (2009) 73005.

[33] B. Delley, From molecules to solids with the DMol3 approach, J. Chem. Phys. 113 (2000) 7756–7764.

[34] D.S. Biovia, Discovery Studio Modeling Environment, Release 2017, Dassault Syst{è}mes, San Diego, CA. (2016).

[35] J.P. Perdew, K. Burke, M. Ernzerhof, Generalized gradient approximation made simple, Phys. Rev. Lett. 77 (1996) 3865.

[36] T. Liang, W.-X. Li, H. Zhang, A first-principles study on the behavior of HCl inside SWCNT, J. Mol. Struct. THEOCHEM. 905 (2009) 44–47.

[37] X. Lu, Z. Deng, C. Guo, W. Wang, S. Wei, S.-P. Ng, X. Chen, N. Ding, W. Guo, C.-M.L. Wu, Methanol Oxidation on Pt3Sn (111) for Direct Methanol Fuel Cells: Methanol Decomposition, ACS Appl. Mater. Interfaces. 8 (2016) 12194–12204.

[38] M. Zhang, R. Yao, H. Jiang, G. Li, Y. Chen, Catalytic activity of transition metal doped Cu (111) surfaces for ethanol synthesis from acetic acid hydrogenation: a DFT study, RSC Adv. 7 (2017) 1443–1452.

[39] D.S. BIOVIA, Discovery studio modeling environment, release 3.5, Accelrys Softw. Inc., San Diego. (2016).

[40] A. Klamt, G. Schüürmann, COSMO: a new approach to dielectric screening in solvents with explicit expressions for the screening energy and its gradient, J. Chem. Soc. Perkin Trans. 2. (1993) 799–805.

[41] J. Tomasi, M. Persico, Molecular interactions in solution: an overview of methods based on continuous distributions of the solvent, Chem. Rev. 94 (1994) 2027–2094.

[42] C.J. Cramer, D.G. Truhlar, Implicit solvation models: equilibria, structure, spectra, and dynamics, Chem. Rev. 99 (1999) 2161–2200.

[43] M.A. Vincent, I.H. Hillier, Accurate prediction of adsorption energies on graphene, using a dispersion-corrected semiempirical method including solvation, J. Chem. Inf. Model. 54 (2014) 2255–2260.

[44] A.J. Mannix, X.-F. Zhou, B. Kiraly, J.D. Wood, D. Alducin, B.D. Myers, X. Liu, B.L. Fisher, U. Santiago, J.R. Guest, others, Synthesis of borophenes: Anisotropic, two-dimensional boron polymorphs, Science (80-.). 350 (2015) 1513–1516.

[45] L. Liu, X. Zhao, H. Sun, C. Jia, W. Fan, Theoretical Study of H2O Adsorption on Zn2GeO4 Surfaces: Effects of Surface State and Structure--Activity Relationships, ACS Appl. Mater. Interfaces. 5 (2013) 6893–6901.

[46] P. Singla, M. Riyaz, S. Singhal, N. Goel, Theoretical study of adsorption of amino acids on graphene and BN sheet in gas and aqueous phase with empirical DFT dispersion correction, Phys. Chem. Chem. Phys. 18 (2016) 5597–5604.

[47] L. Guo, C. Qi, X. Zheng, R. Zhang, X. Shen, S. Kaya, Toward understanding the adsorption mechanism of large size organic corrosion inhibitors on an Fe (110) surface using the DFTB method, RSC Adv. 7 (2017) 29042–29050.

[48] A.N. Chermahini, A. Teimouri, H. Farrokhpour, A DFT-D study on the interaction between lactic acid and single-wall carbon nanotubes, RSC Adv. 5 (2015) 97724–97733.

[49] I.A. Mudunkotuwa, T. Rupasinghe, C.-M. Wu, V.H. Grassian, Dissolution of ZnO nanoparticles at circumneutral pH: a study of size effects in the presence and absence of citric acid, Langmuir. 28 (2011) 396–403.

[50] J.A. Carr, H. Wang, A. Abraham, T. Gullion, J.P. Lewis, L-Cysteine interaction with Au55 nanoparticle, J. Phys. Chem. C. 116 (2012) 25816–25823.

[51] W. Ji, Z. Shen, M. Fan, P. Su, Q. Tang, C. Zou, Adsorption mechanism of elemental mercury (Hg0) on the surface of MnCl2 (1 1 0) studied by Density Functional Theory, Chem. Eng. J. 283 (2016) 58–64.

[52] B. Hammer, J.K. Nørskov, Theoretical surface science and catalysis—calculations and

concepts, in: Adv. Catal., Elsevier, 2000: pp. 71–129.

[53] T. Puzyn, B. Rasulev, A. Gajewicz, X. Hu, T.P. Dasari, A. Michalkova, H.-M. Hwang, A. Toropov, D. Leszczynska, J. Leszczynski, Using nano-QSAR to predict the cytotoxicity of metal oxide nanoparticles, Nat. Nanotechnol. 6 (2011) 175–178.

[54] M.E. Belghiti, A. Dafali, Y. Karzazi, M. Bakasse, H. Elalaoui-Elabdallaoui, L.O. Olasunkanmi, E.E. Ebenso, Computational simulation and statistical analysis on the relationship between corrosion inhibition efficiency and molecular structure of some hydrazine derivatives in phosphoric acid on mild steel surface, Appl. Surf. Sci. (2019).

[55] I.B. Obot, S. Kaya, C. Kaya, Conceptual Density Functional Theory and its Application to Corrosion Inhibition Studies, in: Concept. Density Funct. Theory Its Appl. Chem. Domain, Apple Academic Press, 2018: pp. 195–216.

[56] G. Gece, S. Bilgiç, Quantum chemical study of some cyclic nitrogen compounds as corrosion inhibitors of steel in NaCl media, Corros. Sci. 51 (2009) 1876–1878.

[57] R.H. Albrakaty, N.A. Wazzan, I.B. Obot, Theoretical study of the mechanism of corrosion inhibition of carbon steel in acidic solution by 2-aminobenzothaizole and 2-mercatobenzothiazole, Int J Electrochem Sci. 13 (2018) 3535–3554.

[58] S. Armaković, S.J. Armaković, J.P. Šetrajčić, S.K. Jaćimovski, V. Holodkov, Sumanene and its adsorption properties towards CO, CO2 and NH3 molecules, J. Mol. Model. 20 (2014) 2170.

[59] A. Liu, X. Ren, M. An, J. Zhang, P. Yang, B. Wang, Y. Zhu, C. Wang, A combined theoretical and experimental study for silver electroplating, Sci. Rep. 4 (2014) 3837.

[60] E. Alibakhshi, M. Ramezanzadeh, G. Bahlakeh, B. Ramezanzadeh, M. Mahdavian, M. Motamedi, Glycyrrhiza glabra leaves extract as a green corrosion inhibitor for mild steel in 1 M hydrochloric acid solution: Experimental, molecular dynamics, Monte Carlo and quantum mechanics study, J. Mol. Liq. 255 (2018) 185–198.

[61] G. Gece, The use of quantum chemical methods in corrosion inhibitor studies, Corros. Sci. 50 (2008) 2981–2992.

[62] Y. Gong, Z. Wang, F. Gao, S. Zhang, H. Li, Synthesis of new benzotriazole derivatives containing carbon chains as the corrosion inhibitors for copper in sodium chloride solution, Ind. Eng. Chem. Res. 54 (2015) 12242–12253.

[63] N. Kovačević, A. Kokalj, DFT study of interaction of azoles with Cu (111) and Al (111) surfaces: role of azole nitrogen atoms and dipole--dipole interactions, J. Phys. Chem. C. 115 (2011) 24189–24197.

[64] J.R. Hahn, H.S. Kang, Role of molecular orientation in vibration, hopping, and electronic properties of single pyridine molecules adsorbed on Ag (1 1 0) surface: A combined STM and DFT study, Surf. Sci. 604 (2010) 258–264.

[65] A.S. Rad, Al-doped graphene as a new nanostructure adsorbent for some halomethane compounds: DFT calculations, Surf. Sci. 645 (2016) 6–12.

[66] A.S. Rad, E. Abedini, Chemisorption of NO on Pt-decorated graphene as modified nanostructure media: a first principles study, Appl. Surf. Sci. 360 (2016) 1041–1046.

[67] C.V.P. Lopez, S.R.V. Garc'\ia, N.F. Ramirez, L.G. González, J.L.R. Cerda, Reactive sites influence in PMMA oligomers reactivity: a DFT study, Mater. Res. Express. (2018).